International Journal of Advances in Engineering and Management (IJAEM)
Volume 3, Issue 7 July 2021, pp: 1837-1843 www.ijaem.net ISSN: 2395-5252

Improved Power Control Strategy for Hybrid AC-DC Micro Grids

Payal S. Askar[1], Prof. Pratik Ghutke[2]

[1]*MTech, Integrated Power System, Department of Electrical, Tulsiramji Gaikwad Patil College of Engineering and Technology, Nagpur.*

[2]*Professor, Department of Electrical, Tulsiramji Gaikwad Patil College of Engineering and Technology, Nagpur.*

Submitted: 01-07-2021 Revised: 10-07-2021 Accepted: 13-07-2021

ABSTRACT -
The simulation modelling and control of hybrid AC/DC micro grids are proposed in this article. The micro grid design eliminates multiple reverse switches from an individual AC or DC grid and streamlines electrical system connections to variable regenerative AC and DC sources and loads. Digi's use of power electronic converters to connect to the utility / grid has raised safety concerns. In either grid-tied or autonomous mode, the proposed hybrid AC/DC micro-grid system can be evaluated. Microgrids are being developed using photovoltaic systems, wind turbine generators, and batteries. The AC sub-grid is correctly coordinated with the DC sub-grid, and a control system for converters for sensitive power transmission is created. The MATLAB is imitated by the system.

Index Terms: Energy management, grid control, grid operation, hybrid micro grid, PV system, wind power generation.

I. INTRODUCTION

The power sector faces two major challenges: a) expanding access to energy to areas of the population that are not connected to the grid, and b) increasing demand from areas that are connected to the grid. In the next decade (by 2020), it is expected that RE will account for 20% of global power generation [1]. Wind, sun, biomass, mini-hydro, fuel cells, and micro turbines are all examples of renewable energy sources.

The microgrid can be designed as a power system with power generation, power storage, and loads that normally operate along the main utility grid and can be disconnected and operated autonomously. Microgrids have microscopic origins with an electronic interface. These micro resources are usually placed at micro turbines, PV panels and fuel cells, biomass, biogas customer sites. They are low cost, low voltage with low carbon emission levels. The Power Electronics interface provides the necessary control and flexibility for microgrid.

Depending on locally available energy sources, Hybrid Micro grid systems can be developed often in combination with a storage element to match the available energy with the load. Many combinations are possible depending on local conditions, such as Wind-Diesel, Wind-Bio, Wind- Battery, Hydro-Bio, Wind-Solar, Hydro-Solar etc. Storage Systems includes Fuel Cells, Battery, Super Capacitor, Pump Storage, and Flywheel.

II. PROPOSED HYBRID SYSTEM

Fig.1 shows a hybrid microgrid system configuration where various ac and dc sources and loads are connected to the corresponding dc and ac networks. Renewable hybrid system with PV panels and wind turbines, batteries as an electrical energy storage device, are considered as renewable energy sources. The AC and DC buses are connected by a three-phase transformer and a main two-way electric current converter to exchange power between the DC and AC sides. The transformer helps to move the AC voltage of the main converter to the utility voltage level and to separate the AC and DC grids.

The appropriate MATLAB system will be documented with a Simulink introduction to achieve minimal signal strength analysis of AC / DC micro grid model and IC micro grid modeling. During islanding condition and droop control strategy for individual micro grids. The frequency-droop characteristic and reactive power management voltage- droop characteristic. Revised IC doping control for interfacing DC and AC micro grids is one of two disorder-based decentralized control strategies. Using the proposed droop method, the IC is able to perform power sharing between the two micro grids in the transition from

International Journal of Advances in Engineering and Management (IJAEM)
Volume 3, Issue 7 July 2021, pp: 1837-1843 www.ijaem.net ISSN: 2395-5252

grid-connected to islanding mode as well as during the islanding operation.

This project is aimed to at a two-stage modified droop method for the bidirectional power control of the hybrid AC/DC micro grid droop control strategy for individual AC micro grids and DC micro grids the main idea is to use the locally generated energy reducing the power draw from the grid. By using power consumption control with a drop factor, DC power is stored within an acceptable range. To combine the smart DC grid with the AC grid in order to suppress the DC bus voltage fluctuation using controllable loads and achieving the stabilization control of the AC grid using the grid side converter interlinking the DC and AC micro grid. The main objective is to operate in grid connected or in the islanding modes of operation.

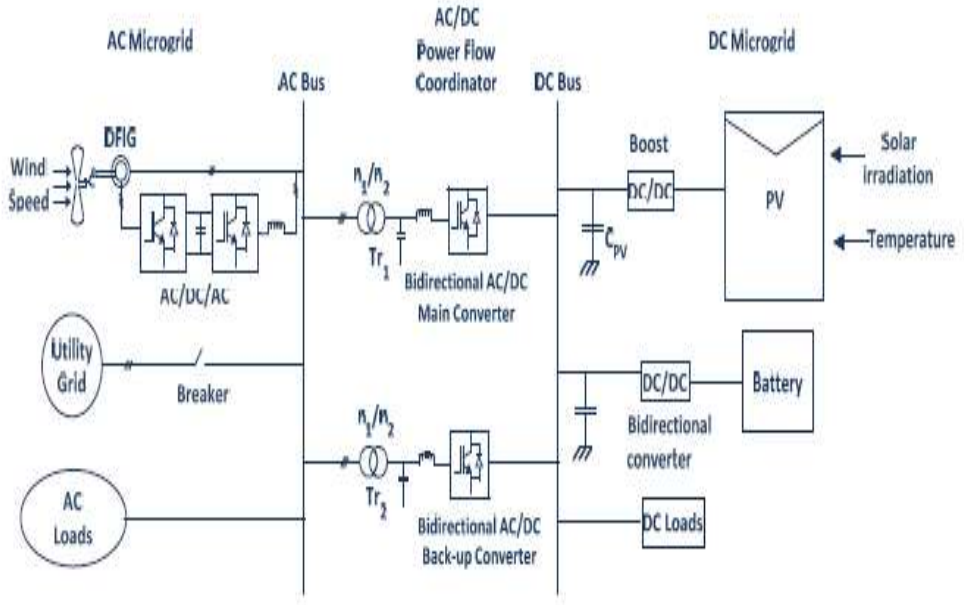

Fig.1 Novel Hybrid ac/dc microgrid system.

The configuration of the hybrid system is shown in Figure where various AC and DC sources and loads are connected to the corresponding AC and DC networks. The figure describes the hybrid system configuration that includes the AC and DC grids. The AC and DC grids have their corresponding sources, loads and energy storage elements, and are interconnected by a 3-phase converter. The AC bus is connected to the utility grid through a transformer logic gate breaker.

III. MATHEMATICAL MODELING AND SIMULINK OF WIND-PV HYBRID MICROGRID

The schematic representation of the hybrid grid is shown in Figure 2. It is designed in MATLAB / Simulink to verify the operation of the system under various load and source conditions. A suspicious feed induction generator of 50 kW rating is connected to the AC bus as an AC source. Forty kW PV series are connected to DC buses as DC sources via a DC / DC boost converter. The 65Ah battery for power storage is connected to the DC bus via a two-way DC / DC converter. Variable DC loads (20 kW - 40 kW) and AC loads (20 kW - 40 kW) are connected to DC and AC buses, respectively. The rated voltages for DC and AC buses are 400 v and 400 v rms, respectively

The three-phase two-way DC / AC main converter with RL-C filter connects the AC bus to the DC bus via an isolation transformer. The wind turbine system consists of a double-to-indicator generator (DFIG) in which the back-to-back AC / DC / AC PWM converter is connected by an AC bus between the slip ring and the rotor. The DFIG wind generation system is attached to the AC bus to simulate AC assets. Variable DC and AC loads are connected to their DC and AC buses so that different loads can be simulated.

The AC and DC buses are connected by a three-phase transformer and a main two-way electric current converter to exchange power between the DC and AC sides. The transformer helps to move the AC voltage of the main converter to the utility voltage level and to separate the AC

International Journal of Advances in Engineering and Management (IJAEM)
Volume 3, Issue 7 July 2021, pp: 1837-1843 www.ijaem.net ISSN: 2395-5252

and DC grids. The booster converter, main converter and bidirectional converter share a common DC bus. For grid tie PV systems, the output of the PV array is connected to a DC-DC booster converter used to perform MPPT functions and to increase the array terminal voltage. The DC link capacitor is used after the DC converter. The LC is connected to the output of a low pass filter inverter to attract high frequency harmonics and prevent them from propagating into the power system grid. The AC bus is connected to the utility grid via a transformer and a circuit breaker. In the proposed system, PV arrays are connected to the DC bus via a boost converter to simulate DC sources. Solar panel production varies mainly due to the level of solar radiation and ambient temperature.

A battery with two-way DC / DC converter is connected to the DC bus as a power storage. The capacitor is connected to the CPV PV terminal to suppress the high frequency waveform of the PV output voltage. The two-way DC / DC converter in discrete mode maintains a constant DC bus voltage by charging or discharging the battery. The modeling of the various additives in a hybrid microgrid is described within the following phase.

1.1. Modeling of Wind Turbine

The aerodynamic model of a wind turbine gives a combination of wind speed and mechanical torque generated by the wind turbine. Mechanical power generated by PM wind turbine rotor:

$$Pm = 0.5\,\rho\,A\,Cp(\lambda,\beta)\,V\omega^3$$

1.2. Modeling of PV Panel

Equivalent circuits of the solar cell are given in figs. The current output of the PV panel is generated by the following equations [8], [11].

$$I_{pv} = n_p I_{ph} - n_p I_{sat}\left[\exp\left(\left(\frac{q}{AkT}\right)\left(\frac{Vpv}{ns} + IpvRs\right)\right) - 1\right]$$

$$Iph = (Isso + ki(T\text{-}Tr)).(S/1000)$$

$$Isat = Irr(T/Tr)3\exp((q\,Egap/kA).(1/Tr\text{-}1/T))$$

Irr = Reverse saturation current

Iph = Photo current

Isat = model reverse saturation current

Ipv = Photovoltaic current

1.3. Modeling of DFIG

d, q, s and r represent the d - axis, q - axis, stator and rotor, respectively. And) angular synchronous velocity and slip velocity, respectively. L denotes the impulse and this is the flux connection. V and I denote voltage and modern-day, respectively. TM Mechanical torque Temp means electromagnetic torque. The voltage equations are as follows - q coordinates of the induction machine in rotation D,

$$v_{ds} = Rsi_{ds} + \frac{d}{dt}\lambda_{ds} - (\omega_e\ \lambda_{qs})$$

$$v_{qs} = Rs\ i_{qs} + \frac{d}{dt}\lambda_{qs} + (\omega_e\ \lambda_{ds})$$

$$v_{dr} = Rr\ i_{dr} + \frac{d}{dt}\lambda_{dr} - (\omega_e\ \lambda_{qr}\ )$$

$$v_{qr} = Rr\ i_{qr} + \frac{d}{dt}\lambda_{qr} + (\omega_e\ \lambda_{qr})$$

$$T_m - T_{em} = \frac{J}{n_p}\frac{d\ \omega_r}{dt}$$

1.4. Modeling and Control of Main Converter

Using the current-controlled voltage source for the main converter, control is implemented to smoothly switch the power between the DC and AC grids and to supply the reactive power distributed to the AC link. [12] Figure 4 shows the manipulation diagram for the primary converter. Two PI controllers are used to achieve real and reactive power control. Whenever the position or load of the source changes, the DC bus voltage is adjusted to stabilize by PI control. When a sudden DC load drop on a DC load causes excessive power, the DC converter is controlled to transmit power from the DC side to the AC side. The active energy absorbed by the capacitor CD leads to the DC link voltage.

Negative error (Vd * -Vd) caused by VD increment produces the most active current reference ID * by PI control. Both the active current ID and its reference ID * are positive. The high positive signal forces the active current ID to increase through the internal current control loop. Therefore, the power overhang of the DC grid can be transferred to the AC side. Similarly, a sudden increase in DC load కారణ causes power loss and Vd falls on the DC grid.

The main converter is controlled to supply power from AC to DC. The positive voltage error (Vd * -Vd) drop leads to an increase in ID * by PI control. Since both ID and ID are negative, the amount of ID increases through the internal current

International Journal of Advances in Engineering and Management (IJAEM)
Volume 3, Issue 7 July 2021, pp: 1837-1843 www.ijaem.net ISSN: 2395-5252

control loop. Consequently, power is transferred from the ac grid to the dc.

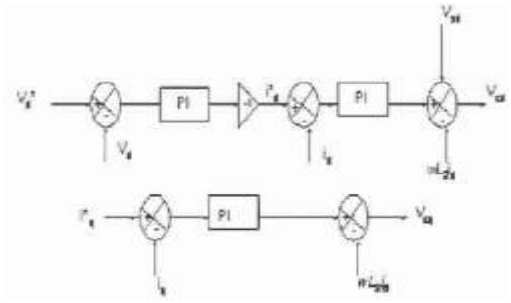

Fig.3 Control diagram of Main Converter

1.5. Modeling & Control of Boost Converter

The boost DC-DC converter is used to increase the input voltage by storing power in the inductor L1 for a certain period of time, and then this voltage is used to increase the input voltage to a higher voltage. Is. The circuit diagram for the boost converter is shown in fig. When switch Q is closed, the input source charges the inductor, diode D1 reverse biased, which is isolated between the input and the output of the converter. When the switch is opened, electricity is stored in the inductor and transferred to the power supply load. The current and voltage equations in a DC bus are as follows

$$V_{pv} - V_T = L_1 \frac{di_1}{dt} + R_1 i_1$$

$$I_{pv} - i_1 = C_{PV} \frac{dV_{pv}}{dt}$$

$V_T = V_d(1 - d_1)$ d_1 is the duty cycle ratio of switch Q.

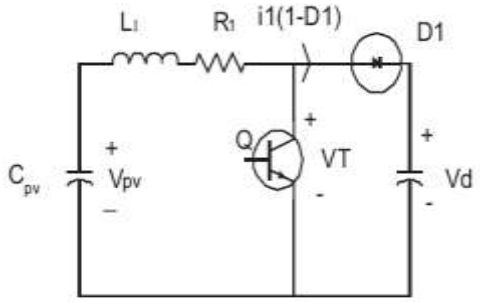

Fig. 4 Boost converter

The reference value of the solar panel terminal voltage is determined by the maximum P&O algorithm to capture the maximum power. Dual loop control for DC / DC booster converter is intended to provide high quality DC voltage. The external voltage loop helps to monitor the reference voltage with zero constant state error and the internal feedback loop helps to improve the dynamic response.

1.6. Modeling and Control of Battery Converter

The battery converter is a two-way DC / DC converter and is designed to provide constant DC-link voltage. The dual loop control scheme for the battery converter is implemented as shown in fig. The current of the injection $I_{in} = i_1 (1 - d_1) - i_{ac} - i_{dc.}]$ should be 1 1 AC The output current of DC. The voltage loop 1 is multiplied before the inner loop is set to the current reference.

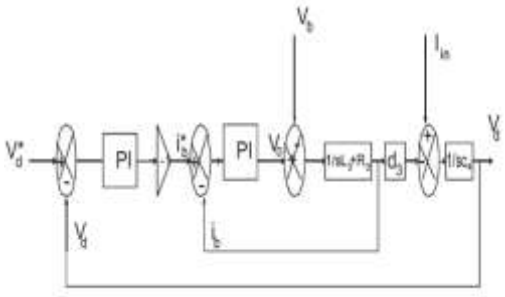

Fig 5 Control of battery converter

The current flowing through the battery is positively defined, where the preset DC link voltage is set to a constant value. Multiplying the positive voltage error (Vdc * -Vdc) by 1 produces a negative IB for the internal current loop, causing the battery to switch from charging to discharge mode and return the Vdc to its predetermined value. That is, due to a sudden increase in load or lack of solar radiation. The battery controller switches from discharge to charging mode in the same control manner. Equations used for battery converter modeling,

$$VD - Vb = L3. \frac{di_t}{dt} + R3\ ib$$

$$VD = Vd.\ d3$$

$$i1\ (1 - d1) - iac - idc - ibd3 = ic = Cd. \frac{dV_d}{dt}$$

IV. SIMULATION RESULTS

The voltage of the solar panel for different solar radiations from 400 W / m2 to 1000 W / m2 to 400 W / m2 in grid-connected mode is shown in Figs. 6 shows. The MPPT algorithm tracks the optimal voltage for 0 to 0.2 seconds.

International Journal of Advances in Engineering and Management (IJAEM)
Volume 3, Issue 7 July 2021, pp: 1837-1843 www.ijaem.net ISSN: 2395-5252

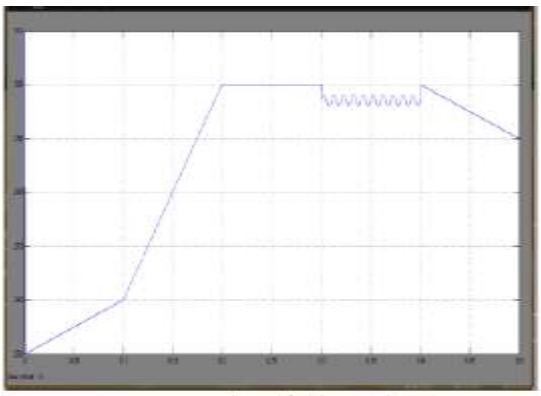

Fig. 6 Voltage of Solar Panel

Fig.7 shows the variation of solar panel power with variable solar radiation and constant load in grid-connected mode. Power from 400 w / m2 to 1000 w / m2 to 400 / m2 with solar radiation from 13.5kW to 37.5kW. Solar radiation varies from 0.1 W / m 2 to 1000 W / m 2 per 0.1 second. Electricity increases with the increase of solar radiation, where the load is constant. Solar radiation decreased to 400 w / m2 in 0.3 seconds, followed by a decrease in energy after 0.3 seconds.

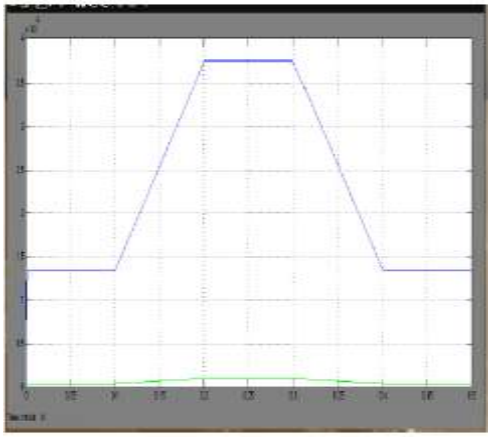

Fig. 7 Power Output of Solar Panel

When the solar radiation level ranges from 1000W / m2 to 0.3 s to 400W / m2 at 0.4 s the voltage (0.2 times the voltage for comparison) and the main side of the current response are shown by the AC side responses Fig 8 shows. KW decreases with constant dc load 20. It can be seen that the energy from the current directions is injected 0.3 seconds in advance from DC to AC grid and reversed after 0.4 seconds.

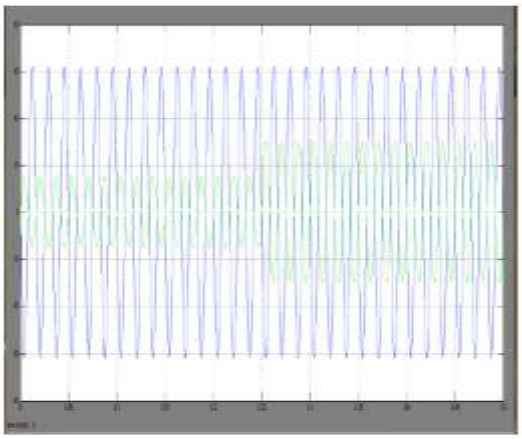

Fig.8 AC side voltage and current of the main converter with constant solar irradiation level and variable dc load

Fig. 9 shows the AC side voltage (voltage time 0.2) and current responses of the main converter when the DC load increases from 0.25 s at 20 kW to 40 kW at 0.25 s with a constant radiation level of 750 W / m2. It may be visible that power is injected from dc to ac grid 0.25 seconds before the contemporary path and reversed after 0.25 seconds.

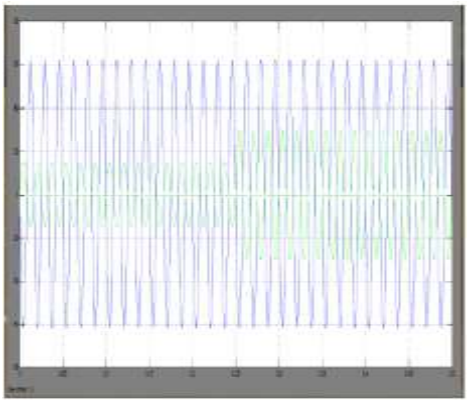

Fig.9 AC side voltage and current of the main converter with constant solar irradiation level and variable dc load.

Fig. 10 shows the voltage response on the DC side of the main converter under the same conditions. The figure shows that the voltage drops at 0.25 C and is quickly corrected by the controller.

International Journal of Advances in Engineering and Management (IJAEM)
Volume 3, Issue 7 July 2021, pp: 1837-1843 www.ijaem.net ISSN: 2395-5252

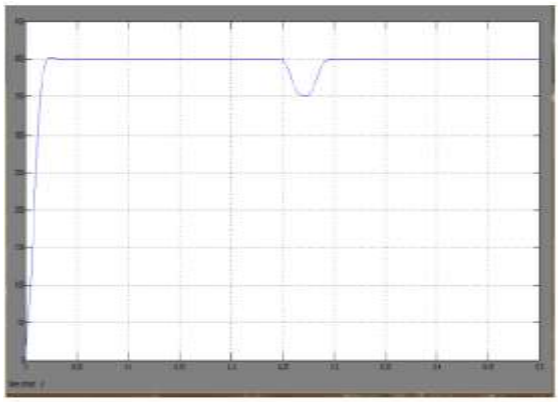

Fig.10 DC bus voltage transient response

1.7. Isolating Mode

Fig.11 suggests the dynamic reaction to the ac aspect of the primary converter while the ac load will increase from 20 kw to 40 kw at 0.3s with a regular wind velocity of 12 m / s. It is clearly shown that the AC grid sends power to the DC grid before 0.3 seconds and receives power from the DC grid after 0.3 seconds. The voltage in the AC bus is kept constant at 326.5 V regardless of load conditions. The nominal voltage and the rated capacity of the battery are decided on as two hundred v and sixty five ah respectively. Fig. 7.10 DFIG additionally indicates the temporary procedure of strength technology, which stabilizes after 0.45 seconds because of mechanical inertia.

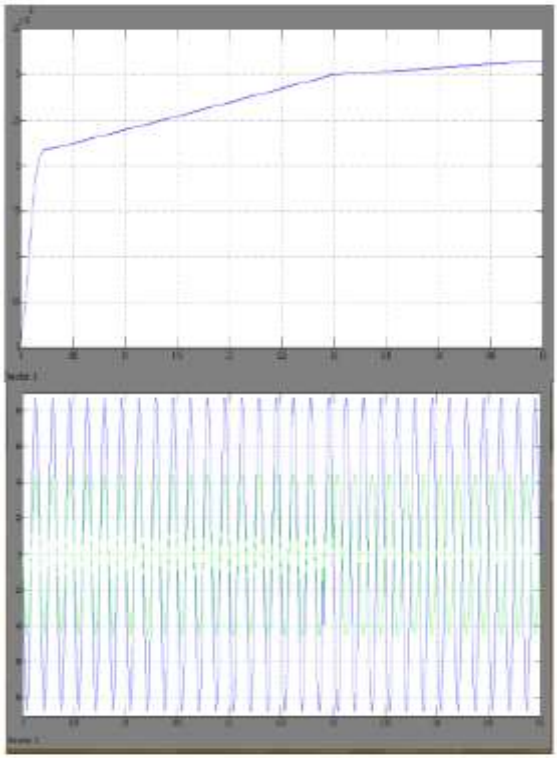

Fig. 11 Upper: output power of the DFIG; Lower: AC side voltage versus current (Voltage times 1/3 for comparison).

Fig.12 indicates the present day and soc of the battery. Figure 13 shows the voltage of the battery. The total force generated is greater than the total load 0.3 s before and less than 0.3 s after the total load. It can be seen from 12 that the battery operates in charging mode after 0.3 seconds due to negative current and positive flow and discharge mode due to negative current. SOC rises and falls before and after 0.3 seconds, respectively.

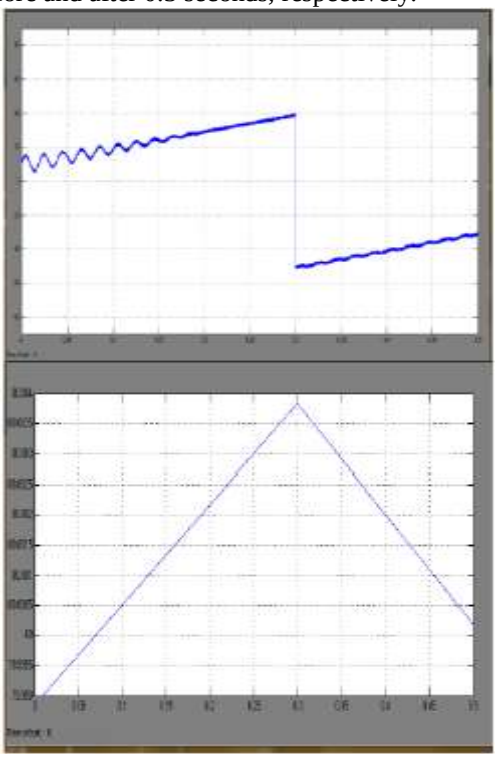

Fig. 12 Battery charging current (upper) and SOC (lower) for the normal case

In case 1 the system is in off-MPPT mode, the DC bus voltage is maintained constant by the boost converter and the AC bus voltage is supplied by the main converter. Fig.14 shows the dc bus voltage, PV output power and battery charging current, respectively, when the dc load is reduced from 20 kW to 0.2 s to 0.2 s with a constant solar radiation level of 1000 W / m2. The battery discharging cutting-edge is kept consistent at 65A. The DC bus voltage is stabilized to 400 V after 0.05 seconds by load change. PV power output comes from the maximum value after 0.2 seconds, which means that the operating modes switch from MPPT to off-MPPT mode. PV output power varies from 35 kW to 25 kW after 0.2 s.

International Journal of Advances in Engineering and Management (IJAEM)
Volume 3, Issue 7 July 2021, pp: 1837-1843 www.ijaem.net ISSN: 2395-5252

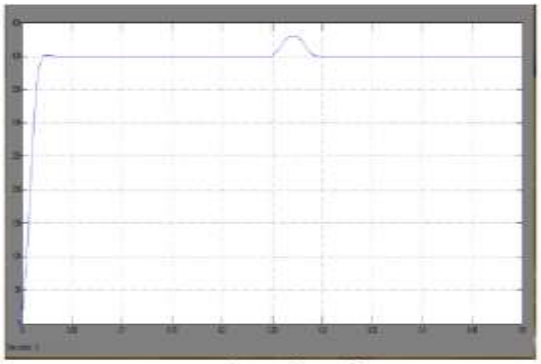

Fig. 14.1 DC bus voltage for Case 1

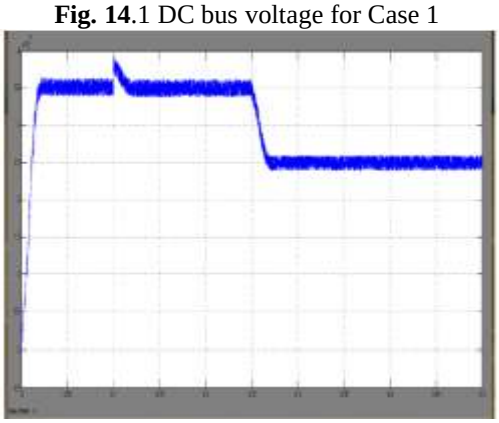

Fig.14.2. PV output power for Case 1

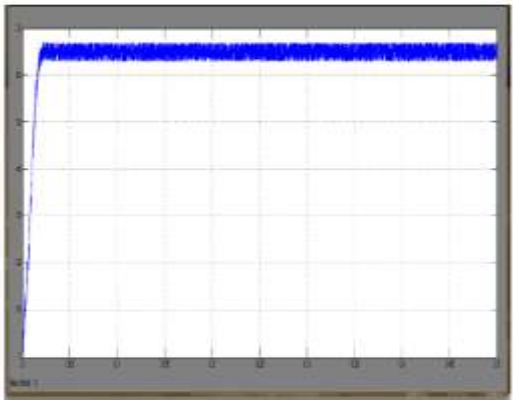

Fig. 14.3. Battery current for Case

CONCLUSION

For power system setup, hybrid AC/DC microgrids have been proposed and hybrid microgrids have been developed in the MATLAB / Simulink environment. The purpose of this study is to hasten the realisation of the major advantages that small-scale distribution generating provides for renewable energy use. To maintain consistent system operation under varying conditions, coordinated control is offered. Although hybrid grids condense the processes of DC / AC and AC / DC conversion to a single AC or DC grid, the installation of hybrid grids based on existing AC-dominated infrastructure has a number of practical issues. Small isolated industrial units having both PV systems and wind turbine generators can use hybrid grids as their primary power source.

REFERENCES

[1]. S. Bose, Y. Liu, K. Bahei-Eldin, J.de Bedout, and M. Adamiak, "Tie line Controls in Microgrid Applications," in iREP Symposium Bulk Power System Dynamics and Control VII, Revitalizing Operational Reliability, pp. 1-9, Aug. 2007.

[2]. R. H. Lasseter, "MicroGrids," in Proc. IEEE-PES'02, pp. 305-308, 2002.

[3]. Michael Angelo Pedrasa and Ted Spooner, "A Survey of Techniques Used to Control Microgrid Generation and Storage during Island Operation," in AUPEC, 2006.

[4]. F. D. Kanellos, A. I. Tsouchnikas, and N. D. Hatziargyriou, "Microgrid Simulation during Grid-Connected and Islanded Mode of Operation," in Int. Conf. Power Systems Transients (IPST'05), June. 2005.

[5]. Y. W. Li, D. M. Vilathgamuwa, and P. C. Loh, Design, analysis, and real-time testing of a controller for multi bus microgrid system, IEEE Trans. Power Electron., vol. 19, pp. 1195-1204, Sep. 2004.

[6]. R. H. Lasseter and P. Paigi, "Microgrid: A conceptual solution," in Proc. IEEEPESC' 04, pp. 4285-4290, 2004.

[7]. F. Katiraei and M. R. Iravani, "Power Management Strategies for a Microgrid with Multiple Distributed Generation Units," IEEE trans. Power System, vol. 21, no. 4, Nov.2006.

[8]. P. Piagi and R. H. Lasseter, "Autonomous control of microgrids," in Proc. IEEE-PES'06, 2006, IEEE, 2006.

[9]. M. Barnes, J. Kondoh, H. Asano, and J. Oyarzabal, "Real-World MicroGrids- an Overview," in IEEE Int. Conf. Systems of Systems Engineering, pp.1-8, 2007.

[10]. Chi Jin, Poh Chiang Loh, Peng Wang, Yang Mi, and Frede Blaabjerg, "Autonomous Operation of Hybrid AC-DC Microgrids," in IEEE Int. Conf. Sustainable Energy Technologies, pp. 1-7, 2010.